Published in final edited form as:
J Neurosci. 2010 April 21; 30(16): 5489–5497. doi:10.1523/JNEUROSCI.6383-09.2010.

Molecular Characterization of Mutations that Cause Globoid Cell Leukodystrophy and Pharmacological Rescue Using Small Molecule Chemical Chaperones

Wing C. Lee[1], **Dongcheul Kang**[1], **Ena Causevic**[1], **Aimee R. Herdt**[1], **Elizabeth A. Eckman**[1], and **Christopher B. Eckman**[1,2]

[1] Department of Neuroscience, Jacksonville, Florida, United States of America

[2] Atlantic Neonatal Research Institute, MidAtlantic Neonatology Associates and Atlantic Health, Morristown, NJ, United States of America

Abstract

Globoid Cell Leukodystrophy (GLD; Krabbe Disease) is an autosomal recessive, degenerative, lysosomal storage disease caused by a severe loss of galactocerebrosidase (GALC) enzymatic activity. Of the more than 70 disease-causing mutations in the *GALC* gene, most are located outside of the catalytic domain of the enzyme. To determine how *GALC* mutations impair enzymatic activity, we investigated the impact of multiple disease-causing mutations on GALC processing, localization and enzymatic activity. Studies in mammalian cells revealed dramatic decreases in GALC activity and a lack of appropriate protein processing into an N-terminal GALC fragment for each of the mutants examined. Consistent with this, we observed significantly less GALC localized to the lysosome and impairment in either the secretion or re-uptake of mutant GALC. Notably, the D528N mutation was found to induce hyper-glycosylation and protein misfolding. Reversal of these conditions resulted in an increase in proper processing and GALC activity, suggesting that glycosylation may play a critical role in the disease process in patients with this mutation. Recent studies have shown that enzyme inhibitors can sometimes "chaperone" misfolded polypeptides to their appropriate target organelle, bypassing the normal cellular quality control machinery and resulting in enhanced activity. To determine if this may also work for GLD we examined the effect of α-lobeline, an inhibitor of GALC, on D528N mutant cells. Following treatment, GALC activity was significantly increased. This study suggests that mutations in *GALC* can cause GLD by impairing protein processing and/or folding and that pharmacological chaperones may be potential therapeutic agents for patients carrying certain mutations.

Keywords

Globoid Cell Leukodystrophy (GLD); Lysosomal Storage Disease; Galactocerebrosidase (GALC); Mutation; Protein misprocessing; Therapeutic

Address Correspondence to: Christopher B. Eckman, PhD, Director of Research and Academic Affairs, Atlantic Neonatology Research Institute and MidAtlantic Neonatology Associates, Morristown Memorial Hospital, 100 Madison Avenue, Morristown NJ 07962. christopher.eckman@atlantichealth.org.

Conflict of Interest Statement: A patent has been filed regarding the use of α-lobeline as a potential pharmacological agent to treat Krabbe Disease.

Introduction

Globoid Cell Leukodystrophy (GLD), also known as Krabbe disease, is a devastating neurodegenerative disorder (Wenger, 2001). It is inherited as an autosomal recessive trait and is characterized by a deficiency in galactocerebrosidase (*GALC*, EC 3.2.1.46) enzymatic activity (Suzuki and Suzuki, 1970). GALC enzymatic activity is predominantly localized in lysosomes, where it is essential for normal catabolism of galactolipids, including a major myelin component, galactocerebroside, and psychosine. GALC deficiency results in abnormal accumulation of psychosine, which is cytotoxic to oligodendrocytes and Schwann cells (Nagara et al., 1986; Tanaka et al., 1988). Loss of these myelin-forming cells causes demyelination in both the central and peripheral nervous systems during early developmental stages (Seitelberger, 1981; Kobayashi et al., 1988). Psychosine accumulation has also been proposed to cause axonal degeneration in the central and peripheral nervous system in the twitcher mouse model of GLD, possibly by altering membrane microdomains (rafts) and some of the associated downstream signaling events (Galbiati et al., 2007; White et al., 2009).

To date, more than 70 disease-causing mutations in the *GALC* gene have been identified, many of which occur in compound heterozygote patterns in patients (De Gasperi et al., 1996; Furuya et al., 1997; Wenger et al., 1997; Fu et al., 1999; Selleri et al., 2000; Wenger et al., 2000; Xu et al., 2006; Lissens et al., 2007). It has been difficult to establish genotype-phenotype relationships for GLD patients given dramatically varied clinical courses, even between individuals with similar or identical genotypes. To more effectively treat patients with diverse disease states, a more detailed understanding of individual *GALC* mutations must be established. The *GALC* gene was cloned in 1993 and the available sequence information provides a framework for studying GLD at the molecular level (Chen et al., 1993; Sakai et al., 1994). The precursor form of GALC contains 669 amino acids and is processed in lysosomes into 2 fragments, an amino-terminal (N-terminal) fragment (50 kDa) and a carboxyl-terminal (C-terminal) fragment (30 kDa) (Nagano et al., 1998). GALC enzymatic activity *in vitro* has been correlated to the amount of the N-terminal (50–53 kDa) fragment present in a partially purified GALC fraction from human urine (Chen and Wenger, 1993). Little is known, however, about the molecular basis of the processing and the endocytosis of the GALC precursor into its lysosomal form. This information may help determine how disease-causing mutations impair the function of GALC at the molecular level, as a large number of disease-causing mutations are located outside of the enzyme's catalytic domain, but nonetheless cause substantial reductions (>95%) in residual enzymatic activity.

Herein, we focused on 3 mutations reported to cause GLD when inherited in the homozygous state: the D528N, I234T, and L629R. The D528N mutation has been reported as the primary mutation responsible for the high incidence of infantile GLD (1 in 100–150 live births) in 2 Moslem Arab villages near Jerusalem (Rafi et al., 1996). The I234T mutation was initially identified in a Greek GLD patient with disease onset at 28 months of age (De Gasperi et al., 1996). The L629R mutation was initially identified in a German GLD patient with symptom onset at 8 years of age (Jardim et al., 1999). These mutations are typically identified in a homozygous state, although the D528N mutation appears to always present with a common polymorphism, I546T, in GLD patients. Expression studies in COS-1 cells show that each of these mutations results in a substantial reduction in GALC activity compared to cells that express wild-type GALC (De Gasperi et al., 1996; Rafi et al., 1996; Jardim et al., 1999). In this study, we analyzed the effects of these mutations on GALC intracellular processing, secretion and uptake, and subcellular localization in mammalian cell lines. Further, we specifically investigated the potential molecular mechanism by which the D528N mutation impairs GALC function. Finally, we describe the

identification and use of the first reported GALC pharmacological chaperone (PC), α-lobeline, which rescues the impaired GALC function of the D528N mutant. We expect that these and similar studies may lead to the development of targeted therapeutics to restore GALC activity in GLD patients.

Materials and Methods

Cloning and construction of human *GALC* expression vectors

We purchased full-length, human, wild-type *GALC* cDNA from OriGene (Rockville, MD). The cDNA was amplified by Phusion high-fidelity DNA polymerase (New England Biolabs, Ipswich, MA) according to the manufacturer's directions. Primers included an *Eco*RI site-containing forward primer (EcoRI-hGalc-START-F, 5′-CTCTCGGAATTCTGGCAACGCCGAGCGAAAGCTATGACTG-3′) and an *Xho*I site-containing reverse primer (XhoI-hGalc-noSTOP-R, 5′-CCTGTTAACTCGAGGCGTGTGGCTTCCACAAGAAAGTTG TC-3′). The amplified cDNA was inserted into the pcDNA4/V5-His A vector (Invitrogen, Carlasbad, CA) using standard procedures. DNA sequencing was performed by the Mayo Clinic Molecular Biology Core Facility to ensure that no random mutations were introduced during the cloning process. Site-directed mutagenesis was performed using the Quikchange II XL site-directed mutagenesis kit (Stratagene, La Jolla, CA). The duplex primers (IDT, Coralville, IA) designed for generating the I234T, D528N, L629R, S530A, and D528N+S530A mutant constructs were:

T701C_forward	5′-GTGGGTTGATGTTACAGGGGCTCATTATCC-3′
T701C_reverse	5′-GGATAATGAGCCCCTGTAACATCAACCCAC-3′
G1582A_forward	5′-CATTACGTGGGCTGCCAATGCATCCAACAC-3′
G1582A_reverse	5′-GTGTTGGATGCATTGGCAGCCCACGTAATG-3′
T1886G_forward	5′-CGCCTCTGGCATGCGGAATGACAAGTC-3′
T1886G_reverse	5′-GACTTGTCATTCCGCATGCCAGAGGCG-3′
T1588G_forward	5′-GTGGGCTGCCGATGCAGCCAACACAATCAG-3′
T1588G_reverse	5′-CTGATTGTGTTGGCTGCATCGGCAGCCCAC-3′
G1582A+T1588G_forward	5′-GTGGGCTGCCAATGCAGCCAACACAATCAG-3′
G1582A+T1588G_reverse	5′-CTGATTGTGTTGGCTGCATTGGCAGCCCAC -3′

WT *GALC* cDNA, subcloned into the pcDNA4/V5-His vector, was used as the template for site-directed mutagenesis. All procedures were performed according to the manufacturer's directions. DNA sequencing was performed on all clones to ensure that no random mutations were introduced and that the desired mutation was present.

Cell culture

COS-1 cells (a monkey kidney, fibroblast-like cell line) and H4 cells (a human, central nervous system-derived cell line) were purchased from ATCC (Manassas, VA). Both cell lines were cultured in Opti-MEM medium supplemented with 5% (v/v) fetal bovine serum (FBS), penicillin (100 IU/ml), and streptomycin (100 μg/ml). OLI-neu, an immortalized oligodendrocyte precursor cell line (Jung et al., 1995), was cultured in Opti-MEM medium supplemented with 5% (v/v) FBS, N2 supplement (1x), 500 pM tri-iodo-thyronine and 5μg/ml insulin. Culture media and all supplements were purchased from Invitrogen, Carlsbad, CA. The cells were maintained in a humidified incubator at 37°C and 5% CO_2. For the GALC uptake study (Figure 2 and Figure 6), OLI-neu cells were seeded at 70% density onto 6-well culture plates pre-coated with poly-L-lysine, and were cultured in reduced serum medium (1% FBS) for one day before adding the GALC-containing media.

Transfection and cell harvesting

Subconfluent (~8×10^5) densities of COS-1 or H4 cells were seeded onto 6-well culture plates one day before transfection. Cell transfection using the Lipofectamine 2000 reagent (Invitrogen, Carlsberg, CA) was performed according to the manufacturer's directions. Plasmids including empty vector (pcDNA4/V5-His A), wild-type *GALC* cDNA and *GALC* containing the disease-causing mutations were purified to transfection grade using an EndoFree plasmid maxi kit (Qiagen, Valencia, CA). For transiently transfected COS-1 cells, cells were harvested at 48 hours, post-transfection. To establish stable, transfected H4 cells, 10% of the transfected cells were passed to new dishes which contained Zeocin™ (400 μg/ml; Invitrogen, Carlsberg, CA) supplemented growth medium. The transfected H4 cells were selected for approximately 3 weeks until Zeocin™-resistant stable colonies were established. Polyclonal stable H4 cell lines expressing wild-type GALC or GALC mutants were either frozen down for storage or propagated for experiments. Harvested cells were prewashed 3 times with phosphate-buffered saline (PBS), pH 7.4 and lysed in the M-Per reagent (Pierce, Rockford, IL) supplemented with a protease inhibitor cocktail (Sigma, St. Louis, MO) for 15 minutes at 4 °C. Cell medium was collected and centrifuged at 500×*g* for 5 minutes before assays. The protein concentration in the lysate was determined by BCA protein assay (Pierce, Rockford, IL) to normalize protein amounts for Western blot and GALC enzymatic activity assays.

Western blot analysis

100 μg of total protein from cell lysates or 20 μl of cell medium was loaded per lane on a 10% Novex Tris-glycine precast gel (Invitrogen, Carlsberg, CA). Protein standards were purchased from New England Biolabs (Ipswich, MA). We performed SDS-PAGE, protein transblotting, and antibody staining using standard methodology (Yager et al., 2002). We used the following antibodies: affinity-purified anti-GALC rabbit polyclonal antibody (CL1475) at 1:1000 (Lee et al., 2005); affinity-purified anti-GALC chicken polyclonal antibody (CL1021AP) at 1:1000; anti-V5 epitope tag antibody at 1:1000 (Abcam, Cambridge, MA). Secondary antibodies included an anti-rabbit IgG horseradish peroxidase-linked antibody (GE healthcare, Piscataway, NJ) and an anti-chicken IgY horseradish peroxidase-linked antibody (Sigma, St. Louis, MO). Both were used at 1:5000 dilution.

GALC enzymatic activity assay

GALC activity assays were performed by modifying the method described previously by Gal et *al*. (Gal et al., 1977). Duplicates from each sample, containing 50 μg total protein or 17.5 μl of cell medium, were mixed with a reaction cocktail (sodium citrate solution at pH 4, sodium taurocholate-oleic acid solution and substrate, 2-hexadecanoylamino-4-nitrophenyl-β-D-galactopyranoside (HNG)). The reaction components were mixed on a 96-well, round-bottom plate and incubated at 37 °C at a time period from 30 minutes to 16 hours depending on the GALC activity of the samples. After incubation, stop solution and absolute ethanol were added and mixed followed by centrifugation (3220×*g*, 10 minutes) to remove precipitates. The absorbance of the supernatant was measured at 410 nm using a SpectraMax M5^e microplate reader (Molecular Devices, Sunnyvale, CA). GALC-specific activity was calculated based on 0.0712 absorbance units measured at 410 nm being equal to 1 nmole of hydrolyzed HNG product in 175 μl.

Identification of α-lobeline as an enzyme inhibitor to GALC

The described GALC enzymatic activity assay was applied as the screening method to identify GALC inhibitors. A cocktail solution containing the reaction buffer, HNG substrate and recombinant human GALC protein (0.1 μg per reaction), was prepared immediately before it was added to tested drugs (GenPlus drug library, Microsource, Gaylordsville, CT)

or vehicle controls (DMSO 4% (v/v)). The final concentration of the drug in each reaction was 0.4 mM and each drug was tested in triplicate wells. The procedures to produce GALC protein were the same as described earlier (Lee et al., 2005). Instead of incubating for 4 hours, the reaction was incubated for 30 minutes. Tested drugs that showed more than a 25% inhibition of GALC activity relative to the control were selected as hits from the primary screen. A dose-response assay was performed to reconfirm the effect of the hits. α-Lobeline (Sigma, St Louis, MO) was prepared as a 20 mg/ml (60 mM) stock solution. It was filtered sterile and stored under -20 °C prior to use.

Confocal immunocytofluorescence analysis

Subconfluent densities (~ 20%) of H4 or H4-GALC cells were seeded on glass cover slips in a 35 mm culture dish 2 days before staining. Under room temperature conditions the cells were washed 3 times with pre-warmed PBS and were fixed in 4% paraformaldehyde for 15 minutes. Blocking solution (PBS at pH 7.4, 0.05% tween-20, 5% goat serum, 0.04% saponin) was added and incubated for 1 hour. Primary antibodies were then added as follows: anti-V5 tag antibody (Abcam, Cambridge, MA) at a 1:100 dilution, anti-GALC antibody, CL1475, at a 1:500 dilution, anti-lamp 2 antibody (BD Pharmingen, San Diego, CA) at a 1:500 dilution, anti-calnexin antibody (Abcam, Cambridge, MA) at a 1:500 dilution and anti-58k golgi protein antibody (Abcam, Cambridge, MA) at a 1:100 dilution. These were allowed to incubate for 2 hours and then were washed 3 times with PBS. Secondary antibodies (Invitrogen, Carlsbad, CA), Alexa Fluor 488 anti-rabbit IgG (for CL1475 and anti-V5 tag antibodies) and Alexa Fluor 488 anti-mouse IgG1 antibody (for anti-lamp2, anti-calnexin and anti-58k golgi protein antibodies), were used at a 1:1000 dilution and allowed to incubate for 1 hour. After secondary antibody binding, the cells on cover slips were washed 3 times with PBS, dried on paper towels, and immediately sealed onto glass slides with a drop of Vectashield mounting media containing DAPI (Vector Lab, Burlingame, CA). The slides were allowed to dry overnight at room temperature before examination. All procedures were carried out in a light-protected environment after secondary antibodies were added. The slides were examined and captured using a Zeiss LSM 510 META confocal microscope. Each image is representative of a field (n = 3) of one out of three independent experiments from each cell line.

Affinity purification by Ni-NTA agarose and in vitro deglycosylation of GALC proteins

Approximately 8×10^6 GALC-transfected, COS-1 cells were lysed in 1 ml of buffer A (50 mM sodium phosphate, 300 mM sodium chloride) containing 1% triton X-100 and 1% protease inhibitor cocktail. The supernatant was collected after centrifugation at 20,000×*g* for 10 minutes at 4 °C. Next, 100 μl of Ni-NTA agarose slurry was added to each 200 μl of supernatant. Binding proceeded at 4 °C for 1 hour on an end-to-end shaker. Agarose beads were washed 3 times with buffer A supplemented with 20 mM imidazole followed by successive centrifugations at 200×*g* for 3 minutes. GALC was released by incubating the beads in 50 μl of buffer A supplemented with 250 mM imidazole. GALC was deglycosylated with endoglycosidase H (Endo H; 1000 U) or peptide: N-glycosidase F (PNG F; 1000 U) (New England Biolabs, Ipswich, MA) at 37 °C for 16 hours. Deglycosylation was stopped by adding an equal volume of 2X Laemmli sample buffer and the reaction was heated to 85 °C for 5 minutes prior to SDS-PAGE and western blotting.

Statistical Analysis

Two-tailed, unpaired t-test was applied to analyze the difference between each mutant GALC groups and WT GALC group (as in Figure 1A and 1D, Figure 2C) and between the D528N GALC and the D528N+S530A GALC groups (as in Figure 6A and 6B). The same statistical analysis was used in the temperature sensitivity study to analyze the effect of sub-physiological temperature on GALC activity in the H4-GALC cell lines (Figure 7A). In

Figure 8, one-way analysis of variance (ANOVA), followed by the Tukey's post-hoc test, was applied to test for differences in GALC activity between α-lobeline treated groups and control group within the same cell line. For the "Uptake Index" shown in Figure 2C and 6B, the data in all groups had passed the Kolmogorov-Smirnov normality test before being analyzed using an unpaired t-test. All data are presented as mean values ± standard error (SE) of at least triplicate samples from representative experiments. Each experiment was independently repeated at least three times.

Results

GLD mutations result in GALC misprocessing and a reduction in residual enzymatic activity

To determine how the GLD mutations influence GALC activity, we generated wild-type (WT) and mutant *GALC* constructs containing D528N, I234T, and L629R mutations fused to a V5 epitope tag followed by a six-histidine (6-His) tag at the C-terminus for analysis. Expression of mutant constructs in COS-1 cells resulted in low, yet detectable, levels of GALC activity in the lysates (Fig. 1A). The WT GALC transfectants exhibited approximately a 47-fold increase in GALC-specific activity compared to the mock transfectants. The D528N, I234T, and L629R mutants had approximately 18%, 7%, and 6% of the GALC-specific activity observed in the WT control, respectively. Identical expression studies were repeated in the human central nervous system derived cell line, H4 (Fig. 1D). Higher GALC activity was observed in WT H4-GALC cells compared to WT COS1-GALC cells. The D528N, I234T, and L629R H4-GALC mutants expressed approximately 6%, 2.6%, and 1.6% of the GALC activity found in the H4-GALC WT control, respectively.

We next sought to determine whether or not these changes in specific activity in the mutant cells were due to changes in processing of the GALC precursor. Western blot analyses were performed on cell lysates using an anti-GALC antibody, CL1475, (Fig. 1B, 1E) and an anti-V5 epitope antibody (Fig. 1C, 1F), that detect the N-terminal and C-terminal ends of GALC, respectively. As expected, WT GALC was normally processed from its 80 kDa precursor form into an N-terminal (50–54 kDa) fragment, as detected by the CL1475 antibody (Fig. 1B, 1E). While the 80 kDa precursor form of GALC was detected in both H4 and COS-1 cells transfected with mutant forms of the enzyme (Fig. 1C, 1F), the 50–54 kDa N-terminal GALC fragment was not detected in any of the 3 mutants examined in either cell type (Fig. 1B, 1E). These data strongly suggest that these mutations alter protein processing. Interestingly, the D528N mutant enzyme also showed an increase in the apparent molecular weight of the 80 kDa precursor form of GALC by SDS-PAGE compared to either of the other 2 mutants or the wild-type enzyme. We used the V5 antibody in this series of experiments (Fig. 1C, 1F) and did not detect the 30 kDa C-terminal fragment of GALC reported by previous studies (Chen and Wenger, 1993).

GLD mutations lead to impaired GALC protein secretion and/or reduced cellular re-uptake

The precursor form of GALC is normally secreted and then taken up by cells via the mannose-6-phosphate receptor for delivery to lysosomes and further processing (Nagano et al., 1998). To determine the influence of GLD mutations on the secretion of GALC, we next performed western blots on the culture media of WT and mutant *GALC*-transfected H4 cells. The GALC precursor (80 kDa) was readily detectable in medium secreted from WT *GALC*-transfected H4 cells (Fig. 2A) and was enzymatically active (Fig. 2C). The I234T and D528N GALC mutants were also secreted by H4 cells at detectable levels, but not by cells transfected with L629R *GALC*, indicating that this mutation causes a severe lack-of-secretion phenotype.

An oligodendrocyte precursor cell line, OLI-neu, was used to examine uptake of WT and mutant GALC secreted by the H4-GALC cells. When the conditioned medium from *GALC*-transfected cells was applied to OLI-neu cells for 24 hours, the cells took up and processed the WT GALC precursor and generated the expected 50–54 kDa N-terminal fragment. The protein band resulting from the uptake and processing of the exogenously added GALC co-migrated with endogenous GALC in OLI-neu cells, resulting in an apparent increase in band intensity compared to the mock control (Fig. 2B). We were unable to detect the 80 kDa precursor form in the cell lysates at the 24 hour time point, suggesting that the precursor is efficiently processed after it enters the cell. The uptake and processing of exogenous WT GALC by OLI-neu cells was associated with a net increase in GALC activity as compared to control (Fig. 2C). The "Uptake Index" is defined as the ratio of GALC activity detected in the cell lysate after uptake divided by the GALC activity in the corresponding input medium. This ratio is then multiplied by 100 and is presented as the "Uptake Index". For WT GALC, the uptake index was 25. As L629R mutant GALC is not secreted from H4 cells at detectable levels, we were unable to analyze this mutation in a similar fashion. The I234T GALC mutant was secreted by H4 cells at levels comparable to WT GALC (Fig. 2A). However, it appears to be mostly enzymatically inactive (Fig. 2C) and was not taken up by OLI-neu cells (Fig. 2B). The secreted form of D528N mutant was detected in the conditioned medium (Fig. 2A) and was enzymatically active (Fig. 2C), but it also was not efficiently taken up by OLI-neu cells (Fig. 2B–C). These results demonstrate that while protein misprocessing appears to be common among the mutations examined, the precise mechanisms differ. These data indicate that, unlike WT GALC, cells expressing I234T, D528N, and L629R mutations are unlikely to supply nearby cells with significant GALC enzymatic activity.

GLD mutations I234T, L629R and D528N impair localization of GALC

To determine if the GLD-causing *GALC* mutations influence the lysosomal localization of the enzyme in cells, we performed double immunofluorescent labeling experiments and confocal image analysis using the CL1475 rabbit anti-GALC antibody to detect both the precursor form and the mature form of GALC, or anti-V5 tag antibody to detect predominantly the precursor form of GALC. For subcellular organelle markers, we used antibodies to detect the lysosomal marker, lysosomal-associated membrane protein 2 (lamp 2), or the endoplasmic reticulum (ER) marker, calnexin, or the golgi apparatus marker, 58k golgi protein. As shown in Figure 3, we detected co-localization of GALC (CL1475 antibody) with lamp 2 in the WT H4-GALC cells, but not in cells expressing any of the 3 GLD mutations examined. Double labeling with anti-calnexin (ER) and the anti-V5 tag antibody to GALC showed co-localization only in the L629R mutant, indicating that the L629R mutant potentially accumulates in the ER, which is entirely consistent with its lack-of-secretion phenotype (Fig. 2A). WT GALC, I234T and D528N mutants were found to colocalize with the golgi marker but not with the ER marker, suggesting that the precursor form of GALC, with or without these mutations, traffics through the ER and reaches the golgi apparatus. However, it appears that only WT GALC is transported to the lysosome to an extent that co-localization studies can readily detect. Collectively, these data indicate that the mutations all influence the level of GALC in lysosomes, where it is needed to maintain normal function.

The D528N mutant is hyperglycosylated in transfected COS-1 cells

The asparagine residue at position 528 of the D528N GALC mutant is flanked in the forward direction by alanine and serine, which combine to fulfill the triplet sequence requirement for a potential N-glycosylation site (Fig. 4). To examine if this mutation-induced, potential N-glycosylation site resulted in aberrant glycosylation of the D528N mutant, we first analyzed the apparent molecular weights of various species of COS-1

expressed GALC by western blot as detected by the anti-V5 tag antibody. Consistent with an increase in glycosylation, we noticed an increase in the apparent molecular weight of the D528N 80 kDa GALC precursor (Fig. 1, 2, and 5B). We also observed an increase in the molecular weight of a 25 kDa C-terminal fragment (Fig. 5C) and a larger band migrating at approximately 170 kDa (Fig. 5A). The C-terminal fragment of GALC was apparent only when the lysates were affinity-purified and concentrated. A similar amount of the C-terminal fragment was found in the D528N cells compared to the WT GALC cells. This suggests that the mutation has no effect on the generation of this fragment. The identity of the larger band may represent a dimer or larger aggregate of the GALC precursor. De-glycosylation with either endoglycosidase H (Endo H) or N-glycosidase F (PNG F) resulted in a decrease in the apparent molecular weights of all 3 mutant bands so that they migrated similarly to the deglycosylated wild-type enzyme (Fig. 5). These data provide strong support that the additional, putative N-glycosylation site created by the D528N mutation is indeed glycosylated.

Enzyme kinetics are not altered in the D528N mutant

To test if the extra N-glycosylation at the D528N residue alters the enzyme kinetics of the mutant GALC protein, K_m and V_{max} values of WT and D528N mutant GALC were determined with various concentration of HNG substrate (from 14 to 900 μM) in 0.1 M sodium citrate buffer, pH 4 at 37 °C using Lineweaver-Burk plots (data not shown). The K_m and V_{max} values of WT GALC from culture medium of H4-GALC cells were 1.35 mM and 0.6 nmol/hour, respectively. The D528N mutant was determined to have a similar K_m and V_{max} values of 1.71 mM and 0.64 nmol/hour, respectively, indicating that GALC enzyme kinetics are not apparently altered by the mutation.

Disruption of the extra D528N N-glycosylation site results in restored protein processing, increased residual GALC activity, increased GALC secretion and uptake, and lysosomal localization

Next, we investigated the impact of the additional N-glycosylation site on GALC enzyme activity, reduced levels of secretion, lack of extracellular uptake and lack of lysosomal localization observed in cells transfected with the D528N mutant. To accomplish this, we designed a GALC-expression construct in which the extra N-glycosylation site created by the D528N mutation was disrupted by a second mutation, S530A (Fig. 4). This double mutant, D528N+S530A, was processed similarly to WT GALC with significant increases in the levels of 50–54 kDa N-terminal fragment detected in cells, as opposed to the D528N mutation alone (Fig. 6A, immnoblot). This was accompanied by a significant increase in enzymatic activity in the double mutant (Fig. 6A, graph). Additionally, there was a significant increase in secreted GALC enzymatic activity of GALC in the H4 cells even though the amount of GALC detected by western blot was not apparently increased (Fig. 6B, table). The uptake efficiency of the double mutant was also increased to a level comparable to that in WT GALC by OLI-neu cells as indicated by the “Uptake Index” (Fig. 6B, table). Finally, the D528N+S530A GALC was observed to co-localize with lamp2 (as shown in yellow color), indicating that lysosomal localization was partially restored (Fig. 6C). These results suggest that the molecular defects in the D528N GALC mutant are likely related, at least in part, to N-glycosylation at the mutation site and that reversing this glycosylation can result in substantial improvements, even though the original mutation is still present in this construct.

The D528N mutant GALC is stabilized and properly processed under reduced temperature

To examine whether or not protein misfolding is involved in the GALC protein misprocessing and impairment of GALC activity in the I234T, L629R, D528N and D528N +S530A mutant cell lines, cells were cultured under physiological (37°C) or reduced (30°C)

temperature for 72 hours, a condition known to facilitate protein folding (Denning et al., 1992; Berson et al., 2000; Vollrath and Liu, 2006). Processing of WT GALC into the 54 kDa N-terminal fragment and associated enzyme activity was significantly decreased by approximately 31% at reduced temperature (Fig. 7A, 7B). This is consistent with reduced temperature not being ideal for normal GALC processing. In contrast, processing of GALC precursor into the N-terminal fragment was apparently increased in D528N mutant when the cells were cultured at reduced temperature (Fig. 7B). This increase in processing was accompanied by a significant 50% increase in GALC activity (Fig. 7A). No significant change in activity was found in I234T, L629R and D528N+S530A mutants (Fig 7A). Collectively, these results suggest that protein misfolding may also be involved in the molecular mechanism by which the D528N mutation impairs the function of GALC.

Identification of α-lobeline to rescue the function of D528N GALC mutant

A novel, therapeutic approach to treat lysosomal storage diseases (LSDs) includes the use of enzyme inhibitors as ligands to protect misfolded, newly synthesized polypeptides from degradation. These enzyme inhibitors, also known as pharmacological chaperones (PCs), have been reported to rescue partial function of mutant lysosomal enzymes that are responsible for the onset of various LSDs (reviewed in part in (Fan, 2008)). To identify potential PCs to treat GLD, we screened for GALC inhibitors with a modified, 96-well microplate *in vitro* enzymatic activity assay (Gal et al., 1977). α-Lobeline, an FDA category 3 drug with a known ability to cross the blood-brain barrier, was identified as a relatively weak inhibitor of GALC (Fig. 8A). To determine if this weak inhibitor might act as a chemical chaperone, we treated the D528N mutant H4-GALC cells with α-lobeline at 60, 120, and 240 μM for 72 hours and analyzed GALC enzymatic activity in lysates and culture media. As a control, the WT GALC cells were also treated and analyzed under the same conditions. The intracellular (lysates) and the extracellular (media) GALC activity in D528N mutant were increased significantly by 52% and 64%, respectively, at the highest α-lobeline dose (Fig. 8C). In contrast, the intracellular GALC activity in WT cells was not changed and the extracellular GALC activity was increased by a more modest 26%, under the same conditions (Fig. 8B). We did not see similar effects with the I234T and L629R mutants, suggesting that the effect of α-lobeline on the D528N mutant was mutation-specific (data not shown) (Sawkar et al., 2005). Our results indicate that α-lobeline preferentially increases the intracellular GALC activity of the D528N mutant, which suggests that α-lobeline has the ability to function as a pharmacological chaperone to rescue the function of this mutant.

Discussion

In this report, we have shown that 3 different mutations in *GALC* result in protein misprocessing (Fig. 1), altered protein secretion and/or re-uptake of the enzyme (Fig. 2), and/or lack of trafficking to lysosomes of the mutant enzyme (Fig. 3). Of the 3 disease-causing mutations we examined, all were produced at the protein level and could be detected as an 80 kDa precursor, but none of the mutants were detected as the processed 50–54 kDa N-terminal fragment. These data clearly indicate that GLD can be caused by protein misprocessing of GALC.

While it may be reasonable to expect a direct correlation of residual GALC enzyme activity with disease phenotype (i.e. a higher residual activity should present a less severe phenotype or later symptom onset), it appears that it is not always the case with GLD. For example, residual GALC activity in both leukocyte and skin fibroblast samples from the patient with the L629R mutation, who was diagnosed with late-onset GLD, is indistinguishable from residual GALC activity in infantile patients who have the most severe form of GLD (Jardim et al., 1999). The I234T mutation, which was also found in a late-onset patient, was confirmed to have an undetectable level of residual activity (De Gasperi et al., 1996). These

observations suggest that in addition to the level of residual GALC activity, genetic background and potentially environmental factors may also contribute to the severity of GLD.

Interestingly, one of the mutations examined, the D528N mutation, appears to create a novel glycosylation site. Disrupting this site by mutating the adjacent amino acid can partially restore enzyme function even though the protein still contains the original mutation (Fig. 6). According to the Human Gene Mutation Database, approximately 142 out of 10047 potential mutations (~1.4%) in 77 out of 577 genes (~13.3%) create new, potential N-glycosylation sites (Vogt et al., 2005). Some of these mutations are linked to pathogenic effects in various inherited diseases such as congenital dysfibrinogenemia (Yamazumi et al., 1989), neonatal Marfan syndrome (Lonnqvist et al., 1996), and type I antithrombin deficiency (Fitches et al., 2001). Similarly, the D528N mutation appears to influence glycosylation, and alter protein processing, secretion, re-uptake and trafficking to lysosomes in a way that reduces GALC function and causes disease.

Previous studies have shown that protein misfolding is a common molecular mechanism that accounts for many monogenetic-inherited disorders, including many LSDs (Butters, 2007; Fan and Ishii, 2007). Temperature-sensitive folding (TSF) mutations, originally found in the tailspike of Phage P22 protein (Yu and King, 1988), has been defined as amino acid substitutions that destabilize intracellular protein folding by kinetically trapping it in an intermediate, nascent polypeptide state at physiological temperature. Under sub-physiological temperature, proteins bearing the TSF mutation can resume folding into its mature form without significant loss of function. To determine if any of the GLD mutations in this study are temperature sensitive, we examined the processing and activity of the GALC mutants at reduced temperature (Fig 7). Consistent with influence of temperature on other TSF mutations, an increase in protein processing to the 54 kDa N-terminal fragment, accompanied by an increase in GALC activity, was found in cells expressing the D528N mutant when cultured under reduced temperature.

Pharmacological chaperones (PCs), often in the form of enzyme inhibitors that bind and stabilize the native conformation of misfolded proteins, are emerging therapeutic agents for protein misfolding diseases. To attempt to determine if PCs might be useful therapeutics for GLD, we tested whether or not α-lobeline, a relatively weak GALC inhibitor, could influence protein processing and enzymatic activity in cells expressing the D528N mutation. α-Lobeline treatment preferentially increased the intracellular GALC activity of the D528N mutant (Fig. 8C) but not WT GALC cells (Fig. 8B) and caused a dose-dependent increase in GALC secretion in the D528N mutant (Fig. 8B). These *in vitro* data suggest that α-lobeline is a potential PC that can partially enhance GALC function in cells carrying the D528N GLD mutation. To validate this same effect *in vivo*, new animal models containing this mutation are needed. Collectively these data indicate that GLD can be caused by protein misfolding/misprocessing and that at least with the D528N mutation, this can be partially corrected through the use of pharmacological chaperones.

Acknowledgments

This work was supported by funding from the Mayo Clinic Foundation for Medical Education and Research and a grant from the National Institute of Neurological Disorders and Stroke (NS44230) to CE. We would also like to acknowledge Ms. Holly Hammond for proofreading the manuscript.

References

Berson JF, Frank DW, Calvo PA, Bieler BM, Marks MS. A common temperature-sensitive allelic form of human tyrosinase is retained in the endoplasmic reticulum at the nonpermissive temperature. J Biol Chem. 2000; 275:12281–12289. [PubMed: 10766867]

Butters TD. Gaucher disease. Curr Opin Chem Biol. 2007; 11:412–418. [PubMed: 17644022]

Chen YQ, Wenger DA. Galactocerebrosidase from human urine: purification and partial characterization. Biochim Biophys Acta. 1993; 1170:53–61. [PubMed: 8399327]

Chen YQ, Rafi MA, de Gala G, Wenger DA. Cloning and expression of cDNA encoding human galactocerebrosidase, the enzyme deficient in globoid cell leukodystrophy. Hum Mol Genet. 1993; 2:1841–1845. [PubMed: 8281145]

De Gasperi R, Gama Sosa MA, Sartorato EL, Battistini S, MacFarlane H, Gusella JF, Krivit W, Kolodny EH. Molecular heterogeneity of late-onset forms of globoid-cell leukodystrophy. Am J Hum Genet. 1996; 59:1233–1242. [PubMed: 8940268]

Denning GM, Anderson MP, Amara JF, Marshall J, Smith AE, Welsh MJ. Processing of mutant cystic fibrosis transmembrane conductance regulator is temperature-sensitive. Nature. 1992; 358:761–764. [PubMed: 1380673]

Fan JQ. A counterintuitive approach to treat enzyme deficiencies: use of enzyme inhibitors for restoring mutant enzyme activity. Biol Chem. 2008; 389:1–11. [PubMed: 18095864]

Fan JQ, Ishii S. Active-site-specific chaperone therapy for Fabry disease. Yin and Yang of enzyme inhibitors. Febs J. 2007; 274:4962–4971. [PubMed: 17894781]

Fitches AC, Lewandowski K, Olds RJ. Creation of an additional glycosylation site as a mechanism for type I antithrombin deficiency. Thromb Haemost. 2001; 86:1023–1027. [PubMed: 11686319]

Fu L, Inui K, Nishigaki T, Tatsumi N, Tsukamoto H, Kokubu C, Muramatsu T, Okada S. Molecular heterogeneity of Krabbe disease. J Inherit Metab Dis. 1999; 22:155–162. [PubMed: 10234611]

Furuya H, Kukita Y, Nagano S, Sakai Y, Yamashita Y, Fukuyama H, Inatomi Y, Saito Y, Koike R, Tsuji S, Fukumaki Y, Hayashi K, Kobayashi T. Adult onset globoid cell leukodystrophy (Krabbe disease): analysis of galactosylceramidase cDNA from four Japanese patients. Hum Genet. 1997; 100:450–456. [PubMed: 9272171]

Gal AE, Brady RO, Pentchev PG, Furbish FS, Suzuki K, Tanaka H, Schneider EL. A practical chromogenic procedure for the diagnosis of Krabbe's disease. Clin Chim Acta. 1977; 77:53–59. [PubMed: 17489]

Galbiati F, Basso V, Cantuti L, Givogri MI, Lopez-Rosas A, Perez N, Vasu C, Cao H, van Breemen R, Mondino A, Bongarzone ER. Autonomic denervation of lymphoid organs leads to epigenetic immune atrophy in a mouse model of Krabbe disease. J Neurosci. 2007; 27:13730–13738. [PubMed: 18077684]

Jardim LB, Giugliani R, Pires RF, Haussen S, Burin MG, Rafi MA, Wenger DA. Protracted course of Krabbe disease in an adult patient bearing a novel mutation. Arch Neurol. 1999; 56:1014–1017. [PubMed: 10448809]

Jung M, Kramer E, Grzenkowski M, Tang K, Blakemore W, Aguzzi A, Khazaie K, Chlichlia K, von Blankenfeld G, Kettenmann H, et al. Lines of murine oligodendroglial precursor cells immortalized by an activated neu tyrosine kinase show distinct degrees of interaction with axons in vitro and in vivo. Eur J Neurosci. 1995; 7:1245–1265. [PubMed: 7582098]

Kobayashi S, Katayama M, Satoh J, Suzuki K, Suzuki K. The twitcher mouse. An alteration of the unmyelinated fibers in the PNS. Am J Pathol. 1988; 131:308–319. [PubMed: 3358457]

Lee WC, Courtenay A, Troendle FJ, Stallings-Mann ML, Dickey CA, DeLucia MW, Dickson DW, Eckman CB. Enzyme replacement therapy results in substantial improvements in early clinical phenotype in a mouse model of globoid cell leukodystrophy. Faseb J. 2005; 19:1549–1551. [PubMed: 15987783]

Lissens W, Arena A, Seneca S, Rafi M, Sorge G, Liebaers I, Wenger D, Fiumara A. A single mutation in the GALC gene is responsible for the majority of late onset Krabbe disease patients in the Catania (Sicily, Italy) region. Hum Mutat. 2007; 28:742. [PubMed: 17579360]

Lonnqvist L, Karttunen L, Rantamaki T, Kielty C, Raghunath M, Peltonen L. A point mutation creating an extra N-glycosylation site in fibrillin-1 results in neonatal Marfan syndrome. Genomics. 1996; 36:468–475. [PubMed: 8884270]

Nagano S, Yamada T, Shinnoh N, Furuya H, Taniwaki T, Kira J. Expression and processing of recombinant human galactosylceramidase. Clin Chim Acta. 1998; 276:53–61. [PubMed: 9760019]

Nagara H, Ogawa H, Sato Y, Kobayashi T, Suzuki K. The twitcher mouse: degeneration of oligodendrocytes in vitro. Brain Res. 1986; 391:79–84. [PubMed: 3513905]

Rafi MA, Luzi P, Zlotogora J, Wenger DA. Two different mutations are responsible for Krabbe disease in the Druze and Moslem Arab populations in Israel. Hum Genet. 1996; 97:304–308. [PubMed: 8786069]

Sakai N, Inui K, Fujii N, Fukushima H, Nishimoto J, Yanagihara I, Isegawa Y, Iwamatsu A, Okada S. Krabbe disease: isolation and characterization of a full-length cDNA for human galactocerebrosidase. Biochem Biophys Res Commun. 1994; 198:485–491. [PubMed: 8297359]

Sawkar AR, Adamski-Werner SL, Cheng WC, Wong CH, Beutler E, Zimmer KP, Kelly JW. Gaucher disease-associated glucocerebrosidases show mutation-dependent chemical chaperoning profiles. Chem Biol. 2005; 12:1235–1244. [PubMed: 16298303]

Seitelberger F. [Demyelination and leukodystrophy at an early age]. Bol Estud Med Biol. 1981; 31:373–382. [PubMed: 7347616]

Selleri S, Torchiana E, Pareyson D, Lulli L, Bertagnolio B, Savoiardo M, Farina L, Carrara F, Filocamo M, Gatti R, Sghirlanzoni A, Uziel G, Finocchiaro G. Deletion of exons 11-17 and novel mutations of the galactocerebrosidase gene in adult- and early-onset patients with Krabbe disease. J Neurol. 2000; 247:875–877. [PubMed: 11151421]

Suzuki K, Suzuki Y. Globoid cell leucodystrophy (Krabbe's disease): deficiency of galactocerebroside beta-galactosidase. Proc Natl Acad Sci U S A. 1970; 66:302–309. [PubMed: 5271165]

Tanaka K, Nagara H, Kobayashi T, Goto I. The twitcher mouse: accumulation of galactosylsphingosine and pathology of the sciatic nerve. Brain Res. 1988; 454:340–346. [PubMed: 3409017]

Vogt G, Chapgier A, Yang K, Chuzhanova N, Feinberg J, Fieschi C, Boisson-Dupuis S, Alcais A, Filipe-Santos O, Bustamante J, de Beaucoudrey L, Al-Mohsen I, Al-Hajjar S, Al-Ghonaium A, Adimi P, Mirsaeidi M, Khalilzadeh S, Rosenzweig S, de la Calle Martin O, Bauer TR, Puck JM, Ochs HD, Furthner D, Engelhorn C, Belohradsky B, Mansouri D, Holland SM, Schreiber RD, Abel L, Cooper DN, Soudais C, Casanova JL. Gains of glycosylation comprise an unexpectedly large group of pathogenic mutations. Nat Genet. 2005; 37:692–700. [PubMed: 15924140]

Vollrath D, Liu Y. Temperature sensitive secretion of mutant myocilins. Exp Eye Res. 2006; 82:1030–1036. [PubMed: 16297911]

Wenger DA, Rafi MA, Luzi P. Molecular genetics of Krabbe disease (globoid cell leukodystrophy): diagnostic and clinical implications. Hum Mutat. 1997; 10:268–279. [PubMed: 9338580]

Wenger DA, Rafi MA, Luzi P, Datto J, Costantino-Ceccarini E. Krabbe disease: genetic aspects and progress toward therapy. Mol Genet Metab. 2000; 70:1–9. [PubMed: 10833326]

Wenger, DA.; Suzuki, Ku; Suzuki, Y.; Suzuki, Ki. Galactosylceramide lipidosis: globoid cell leukodystrophy (Krabbe disease). In: Scriver, C.; BALR; Sly, WS.; Valle, D., editors. The metaboic and molecular bases of inherited disease. New York: McGraw-Hill; 2001. p. 3669-3694.

White AB, Givogri MI, Lopez-Rosas A, Cao H, van Breemen R, Thinakaran G, Bongarzone ER. Psychosine accumulates in membrane microdomains in the brain of krabbe patients, disrupting the raft architecture. J Neurosci. 2009; 29:6068–6077. [PubMed: 19439584]

Xu C, Sakai N, Taniike M, Inui K, Ozono K. Six novel mutations detected in the GALC gene in 17 Japanese patients with Krabbe disease, and new genotype-phenotype correlation. J Hum Genet. 2006; 51:548–554. [PubMed: 16607461]

Yager D, Watson M, Healy B, Eckman EA, Eckman CB. Natural product extracts that reduce accumulation of the Alzheimer's amyloid beta peptide: selective reduction in A beta42. J Mol Neurosci. 2002; 19:129–133. [PubMed: 12212770]

Yamazumi K, Shimura K, Terukina S, Takahashi N, Matsuda M. A gamma methionine-310 to threonine substitution and consequent N-glycosylation at gamma asparagine-308 identified in a

congenital dysfibrinogenemia associated with posttraumatic bleeding, fibrinogen Asahi. J Clin Invest. 1989; 83:1590–1597. [PubMed: 2496144]

Yu MH, King J. Surface amino acids as sites of temperature-sensitive folding mutations in the P22 tailspike protein. J Biol Chem. 1988; 263:1424–1431. [PubMed: 3257215]

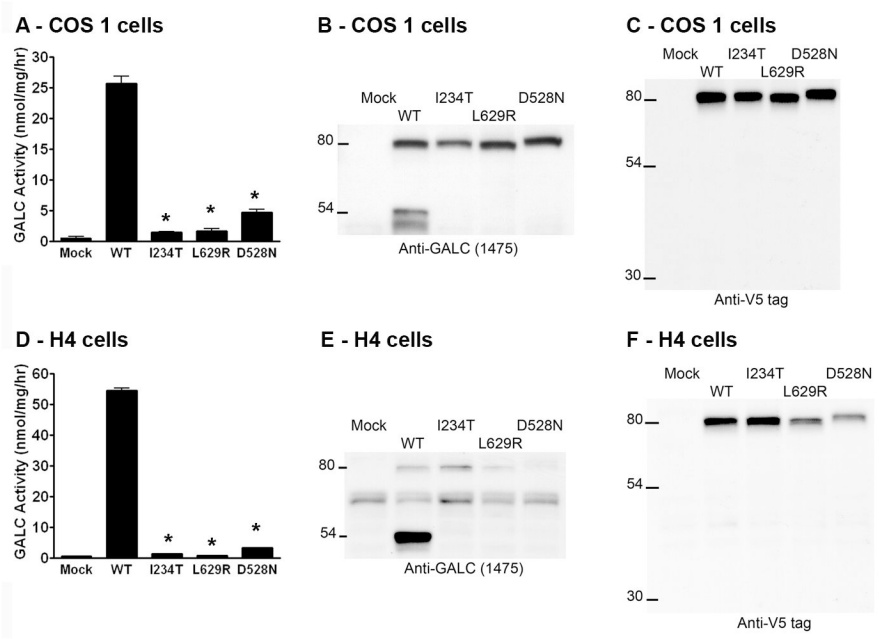

Figure 1. Expression of WT and mutant GALC in mammalian cells

Empty pcDNA4 vector (Mock), human wild type *GALC* cDNA (WT) or GLD-causing *GALC* mutations (I234T, L629R and D528N) were transiently transfected into COS-1 cells **(A–C)**, or stably transfected into H4 cells **(D–F)**. GALC enzymatic activity, measured by *in vitro* colorimetric assay, was significantly reduced in lysates from cells transfected with each mutant GALC, as compared to WT GALC, **P*<0.05 **(A, D)**. The precursor and processed forms of GALC were detected by western blot using the CL1475 rabbit antibody against the amino-terminus of GALC **(B, E)**, and the anti-V5 epitope tag antibody against the carboxyl-terminus of GALC **(C, F)**.

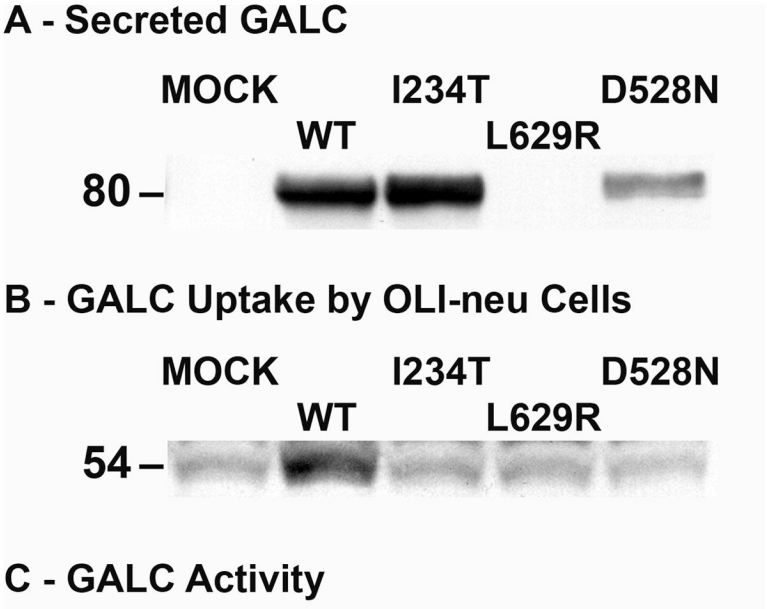

C - GALC Activity

	Mock	WT	I234T	L629R	D528N
Secreted GALC : H4 cells media (nmol/ml/hr)	0	31.2±0.8	0.34±0.01*	0.15±0.01*	8.05±0.2*
GALC Uptake : OLI-neu cells lysate (nmol/mg/hr)	0	7.8±0.13	0	0	0.55±0.07
Uptake Index :		24.9±0.48	0	0	6.87±1.0*

Figure 2. Analysis of the secretion and endocytosis of WT and mutant GALC

Conditioned medium was collected from H4 cells stably transfected with WT *GALC*, mutant *GALC* (I234T, L629R, and D528N), or empty vector (Mock), and was then applied to OLI-neu oligodendrocyte precursor cells for 24 hours to determine the efficiency of GALC uptake.

(A) Western blot (anti-V5 epitope tag) showing detectable levels of GALC protein in conditioned media from WT, I234T, and D528N GALC-transfected H4 cells. Secreted GALC was undetectable in conditioned media from empty vector (mock) transfected and L629R GALC-transfected cells.

(B) Western blot (CL1021AP chicken anti-GALC) of lysates from recipient OLI-neu cells after incubation with conditioned medium from H4 cells expressing WT or mutant GALC.

(C) Summary of GALC activity determined by colorimetric assay from the H4 input media (A) and from the Oli-neu recipient lysates (B). Uptake index is defined as a 100 times the ratio of the GALC activity measured in the cell lysate after uptake compared to the GALC activity in the corresponding input medium. The data in the table represent the mean values ± SE of triplicate samples in each group. GALC secretion and uptake were significantly decreased for each mutant compared to WT GALC, $*P < 0.05$.

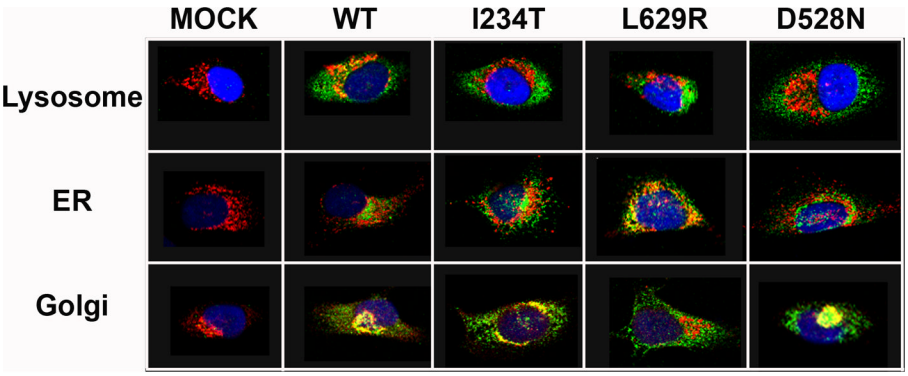

Figure 3. Confocal immunocytofluorescent analysis of GALC in H4-GALC cells

H4 cells (Mock), WT GALC, and mutant (I234T, L629R and D528N) GALC-expressing H4 cells were seeded at subconfluent density on glass cover slips one day before staining. The subcellular localization of GALC was analyzed by co-staining of GALC (CL1475 rabbit anti-GALC antibody) and lamp 2 for lysosomes, costaining of GALC (anti-V5 antibody) and calnexin for ER, and costaining of GALC (anti-V5 antibody) and 58k golgi protein for golgi apparatus. GALC and the organelle markers were illustrated in green and red colors, respectively. Nuclei were labeled with DAPI and illustrated in blue color. Yellow color indicates co-localization of GALC with the organelle markers. All images were captured in 40x magnification using a Zeiss LSM 510 META confocal microscope.

Figure 4. Amino acid sequences near the D528N mutation in GALC

The aspartic acid residue (D) at position 528 was substituted by an asparagine residue (N), which creates an extra N-glycosylation site in the D528N GALC mutant. A double mutant, D528N + S530A, was generated to disrupt the extra N-glycosylation site created by the D528N mutation by replacing the serine residue at position 530 with an alanine residue. A construct containing the S530A mutation only was also generated for an assay control.

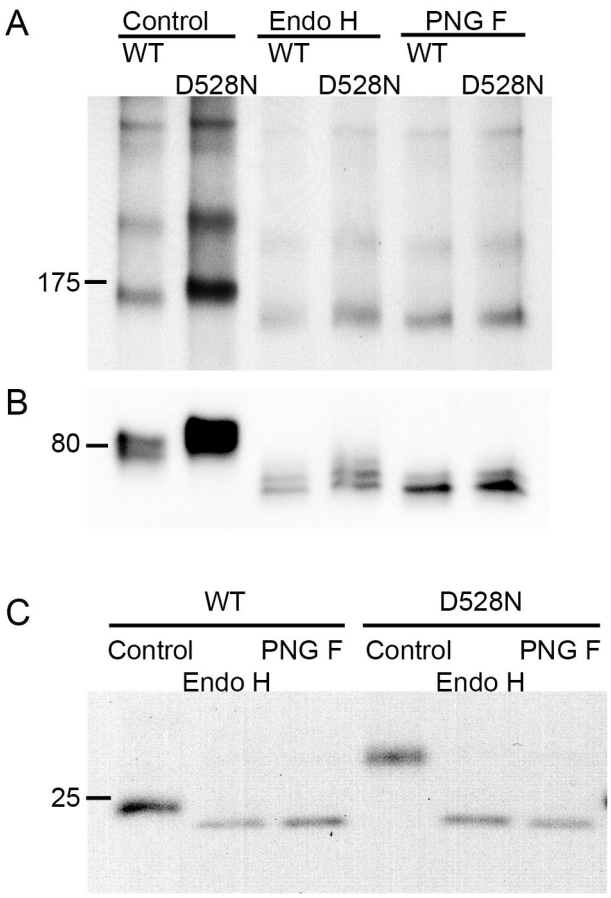

Figure 5. Western blot analysis of the hyperglycosylated D528N GALC mutant overexpressed in COS-1 cells

"Polymeric" GALC **(A)**, monomeric GALC precursors **(B)** and carboxyl-terminal GALC fragments **(C)**, were purified and analyzed without treatment (control) or following deglycosylation by endoglycosidase H (Endo H) or by peptide: N-glycosidase F (PNG F).

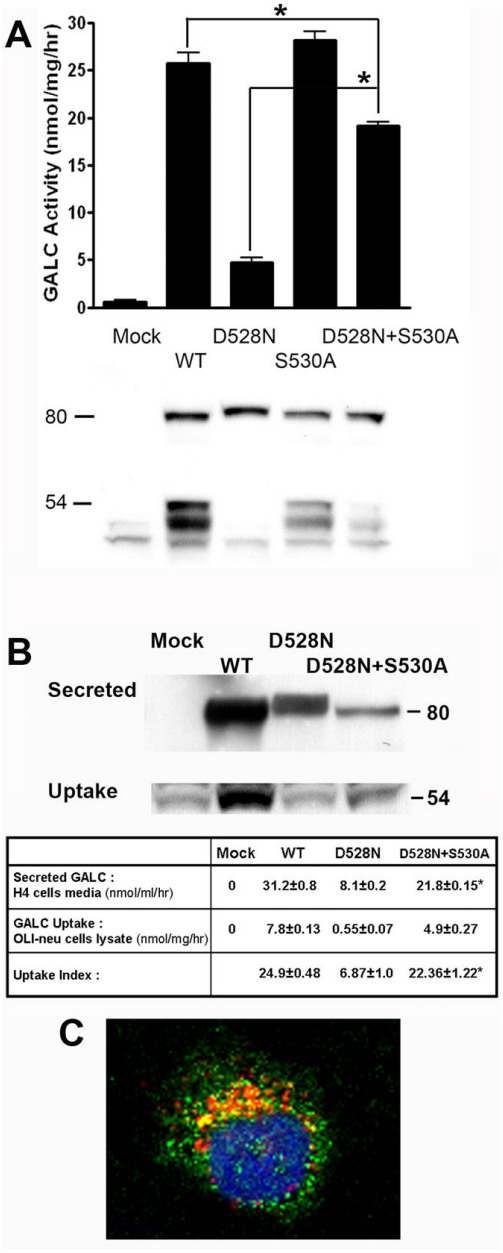

	Mock	WT	D528N	D528N+S530A
Secreted GALC : H4 cells media (nmol/ml/hr)	0	31.2±0.8	8.1±0.2	21.8±0.15*
GALC Uptake : OLI-neu cells lysate (nmol/mg/hr)	0	7.8±0.13	0.55±0.07	4.9±0.27
Uptake Index :		24.9±0.48	6.87±1.0	22.36±1.22*

Figure 6. Expression study of D528N mutant GALC in the presence or absence of glycosylation at position 528

Partial rescue in D528N GALC function, processing, secretion, endocytosis and lysosomal localization was observed in the absence of the glycosylation motif that is introduced with the D528N mutation. **(A)** GALC activity in lysates from COS-1 cells transfected with empty vector (Mock), WT or mutant *GALC* (D528N, S530A or D528N+S530A) **(Upper, graph)**. Data plotted represent the mean ± SE of at least triplicate samples in each group. GALC activity was significantly increased in cells transfected with the double mutant D528N +S530A, compared to the D528N mutant alone, **P*<0.05. The same lysates were analyzed by western blot using the CL1475 rabbit anti-GALC antibody **(Lower, immunoblot). (B)** H4 cells stably transfected with WT and mutant GALC (D528N or D528N+S530S) were used to determine the influence of glycosylation on GALC secretion and uptake.

Conditioned medium from the transfected H4 cells was applied to OLI-neu cells for 24 hours. Media containing the secreted GALC protein **(B, upper immunoblot)** and lysates from recipient OLI-neu cells **(B, lower immunoblot),** were analyzed by western blot using the anti-V5 antibody and the chicken anti-GALC antibody, CL1021AP, respectively. GALC activities from the input cell medium and from the recipient OLI-neu cell lysate were determined and summarized in table format **(B, table)**. Uptake index is defined as a 100 times the ratio of the GALC activity measured in the cell lysate after uptake compared to the GALC activity in the corresponding input medium. The data in the table represent the mean ± SE of triplicate samples in each group. *$P < 0.05$, comparison between the D528N GALC and the D528N+S530A GALC within the same row. **(C)** The subcellular localization of the D528N+S530A mutant GALC expressed in H4 cells was examined by confocal microscopy. Localization of GALC in lysosomes was analyzed by double immunofluorescent staining using CL1475 rabbit antibody against GALC and anti-lamp 2 to label lysosomes, respectively. GALC is in green. Lamp 2 is in red. Nucleus (dapi) is in blue. Magnification equals to 40x. The images are representative image of a field (n = 3) of one out of three independent experiments.

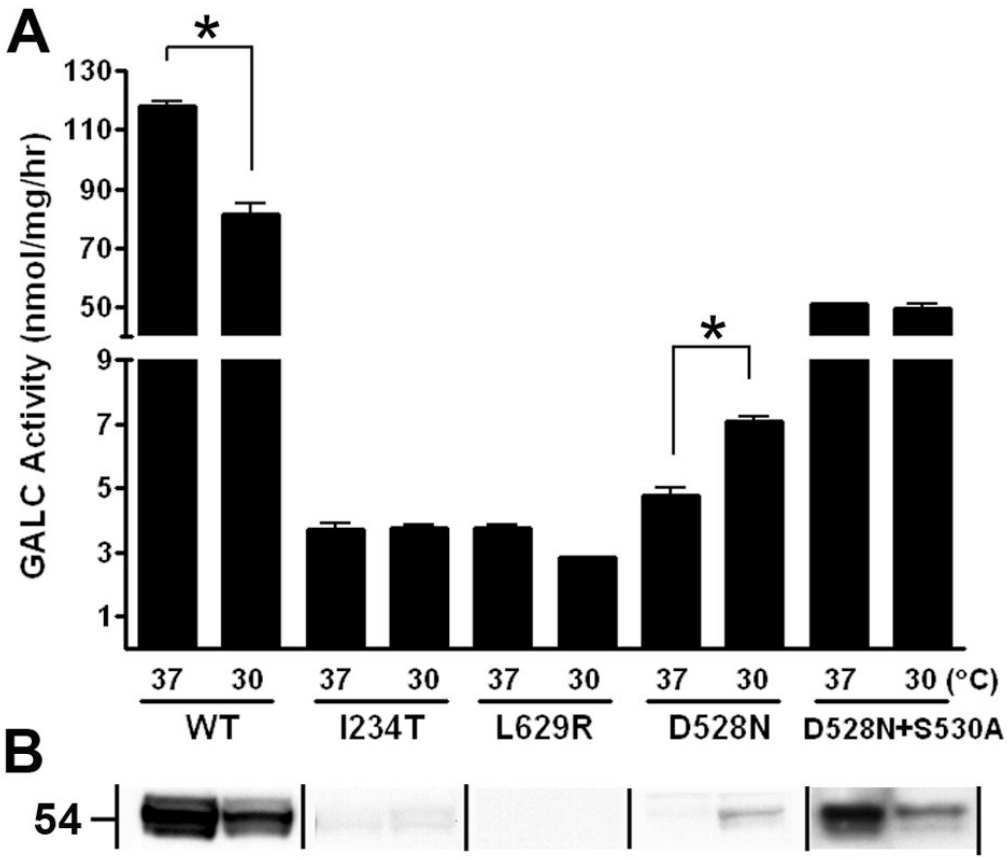

Figure 7. Activity and processing of GALC proteins in H4 cells under sub-physiological temperature

WT and mutant *GALC* (D528N, I234T, L629R and D528N+S530A) transfected H4 cells were cultured at 37°C or 30°C for 72 hours. **(A)** GALC enzymatic activity in lysates was determined by *in vitro* colorimetric assay. Data shown represent the mean ± SE of at least triplicate samples in each group, **P*<0.05. **(B)** Processed amino-terminal GALC fragments (50–54 kDa) from cell lysate were analyzed by western blot using the chicken anti-GALC antibody, CL1021AP.

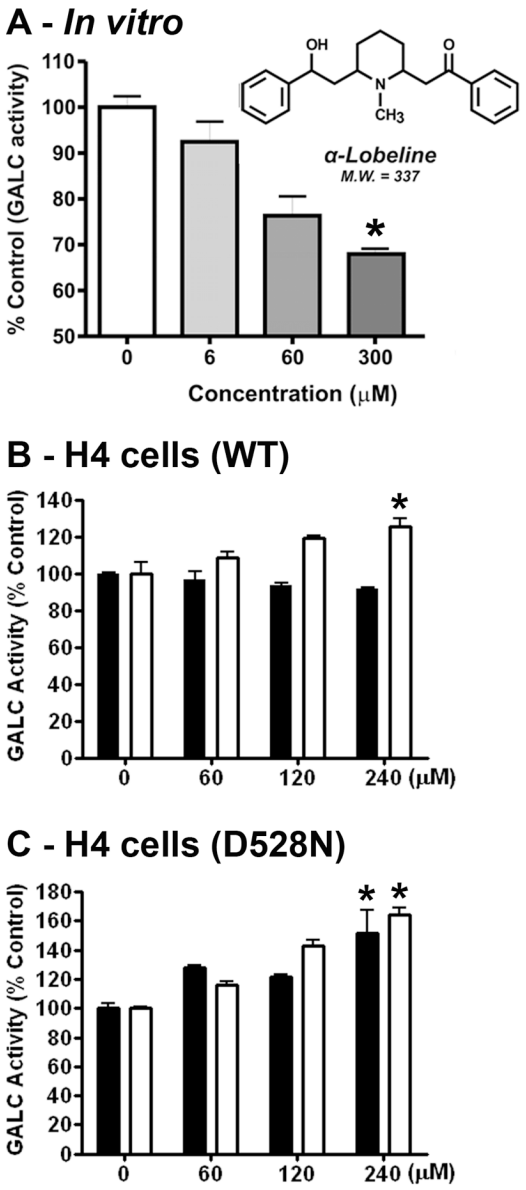

Figure 8.

Effect of α-lobeline on human GALC *in vitro* and in H4 cells expressing WT and mutant *GALC* (I234T, L629R and D528N). **(A)** The inhibition of recombinant GALC by α-lobeline was analyzed using an *in vitro* colorimetric enzymatic activity assay. **(B–C)** H4 cells expressing WT GALC **(B)** or D528N GALC **(C)** were treated with different concentrations of α-lobeline (60 to 240μM) for 72 hours. GALC enzymatic activity in the lysates (black bars) and in the culture media (white bars) was analyzed. Data shown represent the mean ± SE of at least triplicate samples in each group. Statistical analysis was performed by one-way ANOVA test, followed by the Tukey's post-hoc test, **P*<0.05.